

OPTIMIZING IDLER DIAMETER

By

Ronald Lynch
RJLynch & Associates, LLC
USA

ABSTRACT

The idler is probably the most common roller in web handling, but it is one of the least studied. It influences both the highest and lowest tension we can run, and can defeat the most sophisticated tension control schemes. Inertia and bearing drag both upset tension during transient conditions. Idler diameter is one variable that can affect both. Too small a diameter can result in wrinkles caused by deflection, or web damage from bending stress. Too large an idler can result in loss of traction from air entrainment and unnecessarily high equipment cost. Hopefully, there is a diameter that can satisfy all requirements. This paper looks at several factors that must be considered while selecting the best diameter for idlers to minimize their impact on the web path.

NOMENCLATURE

| | |
|-------------------|--|
| A | Linear acceleration of web, m/s^2 |
| E | Young's modulus of shell, N/m^2 |
| J | Rotational moment of inertia, $kg\cdot m^2$ |
| h_a | Air film thickness, m |
| h_w | Web thickness, m |
| k | SI natural frequency constant |
| l | Idler shell length, m |
| m | Rotating mass of idler, kg |
| P | Resultant tension force on idler, N |
| $\Delta T, Drag$ | Tension difference across an idler, N |
| ΔT_b | Tension difference due to bearings, N |
| ΔT_i | Tension difference due to inertia, N |
| ΔT_{peak} | Total tension difference near the end of acceleration, N |
| T_n | Tension on web in span "n", force, N |
| V | Velocity of web, m/s |
| w | Idler shell wall thickness, m |

| | |
|------------|--|
| α | Angular acceleration, rad/s ² |
| β | Total wrap angle on roller, rad |
| γ | Idler dynamic torque, N-m/rad/s |
| η | Dynamic viscosity of air, 18.3x10 ⁻⁶ N-sec/m ² |
| θ | Angular position, rad |
| μ | Coefficient of friction |
| ρ | Idler shell material density, kg/m ³ |
| τ | Idler static-starting torque, N-m |
| ω | Angular velocity, rad/s |
| Subscripts | |
| b | Bearing related |
| i | Inertia related |
| n | Span number |

INTRODUCTION

Idler bearing drag and idler inertial drag work together to upset web tension during acceleration and deceleration. Bearing drag consumes a portion of the web's tension and creates a tension difference, ΔT_b , across an idler that increases and decreases with web velocity. During acceleration, the idler's rotating inertia creates an additional drag, ΔT_i , which adds to the bearing drag torque. It disappears during steady state and can reappear during deceleration as a negative, overrunning load, $-\Delta T_i$, driving the web forward.

Figure 1 shows a simple unwind zone with parent roll, two plain idlers, a tension measuring idler, and lastly, a driven roller.

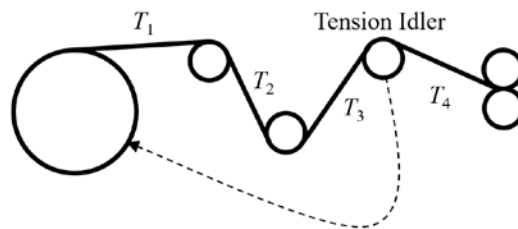


Figure 1 – An Unwind Zone with a Parent Roll, Three Idlers, and a Driven Roller

Figure 2 shows the tension in each span as the web accelerates, runs at steady speed, and then decelerates. Assuming all spans start at the target tension, we see a sudden difference in tension develop across each idler due to the idler's static bearing drag and the imposition of the idler's inertial drag as the web starts to accelerate. At constant acceleration, the inertial drag will remain the same, but the bearing drag and tension difference will increase across the idlers as the velocity increases. A perfect tension control system will be able to keep the resultant tension force, P , between spans 3 and 4 perfectly constant at the tension target; however none of the spans are actually at that value. Span 4's tension will be above the target by approximately half of the total bearing and inertial drag, while span's 3, 2, and 1's tension will be lower than the target, each reduced by the accumulated bearing and inertial drag between it and the driven roller.

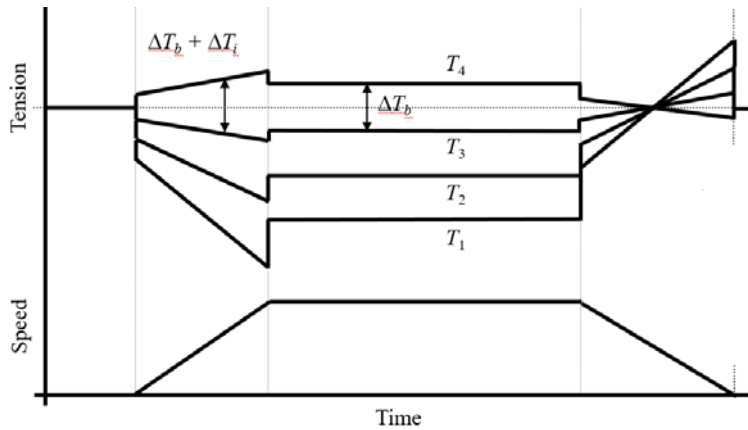


Figure 2 – Tension Distribution across the Four Spans Shown in Figure 1

We see that the lowest tensions occur just before the end of acceleration where the web is near its steady state velocity. Here, the bearing drag is at its greatest value and the inertial drag has not yet disappeared. At the end of acceleration, the inertial drag disappears leaving the bearing drag as the sole contributor to the tension difference across each idler. At the start of deceleration, inertia can reappear as an overrunning load increasing the tension in spans 1, 2, and 3, and pushing web into span 4 lowering its tension. It is possible that near the end of deceleration, span 1 will see the highest tension and span 4 will see its lowest. The extremes of both high and low tension happen near the end of acceleration and deceleration and are caused by the combined effect of idler bearing drag and inertial drag. It is during these times of peak high and low tension that tension related problems are likely to occur.

Similar bearing and inertial drag transients occur in accumulators, dancers, draw control zones, and tension control zones containing one or more idlers. The magnitude of the changes depends on the design and number of idlers, the acceleration rate, and the final velocity.

If the driven roller following span 4 is the pacer roller for the path, the upset in tension will be seen in all downstream spans. If the driven roller is the primary process roller, it will see the transients directly.

Figures 3 and 4 show a more dramatic transient at the pacer or process roller created by moving the tension idler to the first idler in the zone.

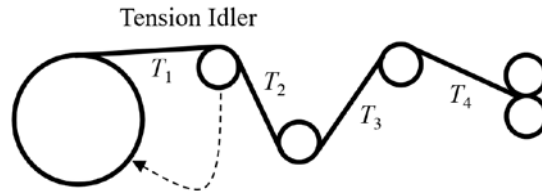


Figure 3 –Tension Idler Upstream

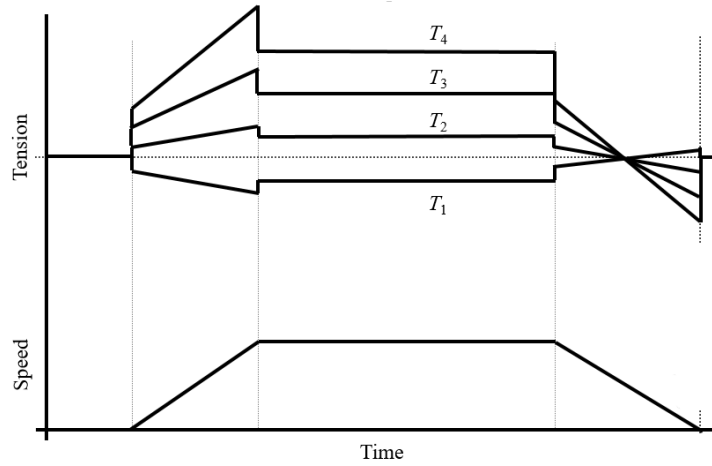


Figure 4 - Tension Distribution Resulting from Figure 3's Arrangement

In both configurations, the highest and lowest tensions seen by the web, and the off target errors, are the result of bearing and inertial drag. Minimizing their combined affect can result in a more stable web path, fewer tension related errors, and can allow running at lower tension.

OPTIMIZING BEARING AND INERTIA DRAG

In its simplest form, idler bearing drag torque can be described as a linear relationship with angular velocity and modeled as

$$Torque_{bearing} = \tau + \gamma\omega \quad \{1\}$$

where τ is the static or starting torque and γ is the increase with rotational velocity.

This can be restated in terms of linear velocity and the tension difference across the idler as

$$\Delta T_b = \tau r_o + \gamma W / r_o^2 \quad \{2\}$$

From this, we can see that increasing the idler radius will reduce the tension difference across the idler caused by bearing drag torque. The inertial drag torque during acceleration is

$$Torque_{inertia} = J\alpha \quad \{3\}$$

The idler's mass moment of inertia depends on its design, but in its simplest form for a hollow shell idler can be reduced to

$$J = mr_o^2 \quad \{4\}$$

where r_o is the outer radius of the idler and the rotating mass is concentrated at this radius.

Formulas 3 and 4 can be combined and can also be restated in terms of the tension difference across the idler and the linear acceleration to become

$$\Delta T_i = mA \quad \{5\}$$

Assuming most mass is in the outer rotating shell of a hollow idler, mass can be restated in the formula in terms of radius, wall thickness, length and density as

$$\Delta T_i = \pi (r_o^2 - (r_o-w)^2) l \rho A \quad \{6\}$$

For idlers, we normally think of "low inertia" as better and this can be achieved by decreasing the radius, wall thickness, or density, i.e., decreasing the rotating mass.

The formulas 2 and 6 can be added to show the total tension difference, ΔT_{peak} , seen across the idler as a function of its properties, linear velocity and linear acceleration.

$$\Delta T_{peak} = \tau r_o + \gamma V / r_o^2 + \pi (r_o^2 - (r_o-w)^2) l \rho A \quad \{7\}$$

The highest total drag occurs near the end of acceleration when velocity and bearing drag are at their highest and the inertial drag is still present. Figure 5 is a plot of formulas 2, 6 and 7 for the "typical" idler properties shown in Table 1. It shows the bearing, inertial and total drag near the end of acceleration as a function of radius.

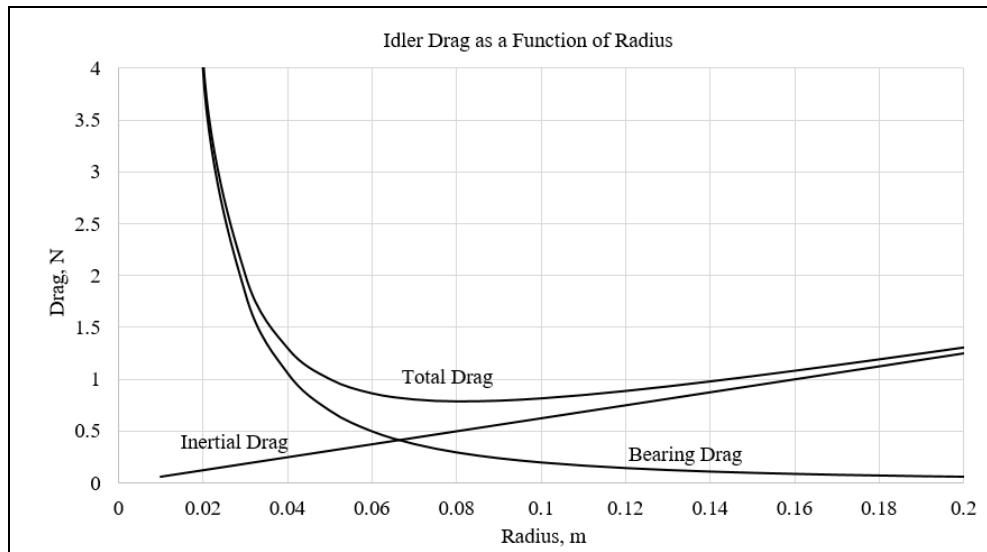


Figure 5 – Idler Drag as a Function of Radius

At small radii, the inertial drag is low, but the rotational velocity is high creating high bearing drag. At large radii, there is low rotational velocity and bearing drag, but higher inertial drag. For the example values in Table 1, the lowest total drag of 0.79 N occurs at a radius of approximately 0.082 m. Higher acceleration or higher density will raise the right side of the plot and shift the optimum diameter to the left. Increased bearing drag or higher velocity will shift it to the right.

| | | | |
|------------|----------|--------------------|--------------------------|
| $l =$ | 1 | meters | idler shell length |
| $w =$ | 0.0025 | meters | shell wall thickness |
| $\rho =$ | 1600 | kg/m ³ | material density |
| $A =$ | 0.25 | m/sec ² | linear acceleration |
| $V =$ | 5 | m/sec | linear velocity |
| $\alpha =$ | 0.005 | N-m | bearing static drag |
| $\gamma =$ | 0.0003 | (N-m)/sec | bearing viscous drag |
| $P =$ | 50 | N/m | resultant web load |
| $k =$ | 9.87 | | SI natural freq const |
| $E =$ | 7.00E+10 | N/m ² | Young's modulus of shell |

Table 1 – Typical Idler Values for a Generic Carbon Composite Idler

DEFLECTION

An important factor in selecting roller diameter is deflection under load. Deflection appears as either a misalignment or steering affect and is a common cause for web wrinkling and mistracking. For a simply supported, centered, dead shaft idler, the mode of deflection is sag of the shell between its support bearings.

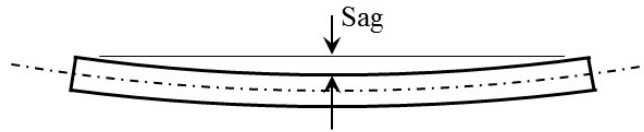


Figure 6 – Roller Sag

The maximum acceptable sag at the midpoint of a roller for general applications is 0.00015 m of sag per meter of length. For a simply supported hollow tube idler, the moment of inertia and maximum sag are calculated using

$$I = \pi(r_o^4 - r_i^4)/4 \text{ and } Sag = 5Pl^4/(384EI) \quad \{8\}$$

Using the values in Table 1, the deflections for several radii are shown in Table 2.

| | | | | | | | | | | |
|-----------|----------|----------|----------|----------|----------|----------|----------|----------|----------|----------|
| Radius, m | 0.04 | 0.045 | 0.05 | 0.055 | 0.06 | 0.065 | 0.07 | 0.075 | 0.08 | 0.085 |
| Sag, m | 0.000201 | 0.000139 | 0.000101 | 0.000075 | 0.000058 | 0.000045 | 0.000036 | 0.000029 | 0.000024 | 0.000020 |

Table 2 – Deflection as a Function of Radius

For the roller properties described above, any roller greater than 0.045 m radius will satisfy this requirement. A 0.045 m radius idler designed as in Table 1 will have 1.13 N of peak drag; 40% more peak drag than the 0.79 N of a similarly designed idler with 0.082 m radius. Its steady state drag will be 0.85 N vs. 0.28 N for a 0.082 m idler; 300% higher. The minimum diameter for sag is not the best choice to minimize the peak or steady state tension difference across the idler.

WEB BENDING RADIUS AND DIFFERENTIAL STRAIN

A web bending over the radius of a roller experiences a strain profile through its thickness and has a neutral bending axis somewhere between its surfaces. See figure 7.

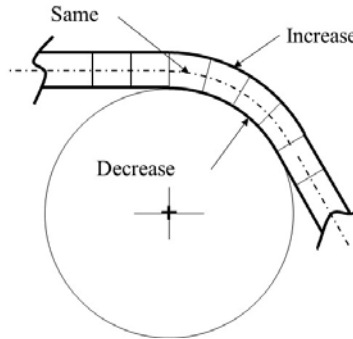


Figure 7 – Web Bending Strain over a Roller

The strain difference between the inside surface and outside surface of the web is approximately.

$$\Delta\varepsilon \approx h_w/r_o \quad \{8\}$$

A 1 mm thick web on 100 mm radius roller will have approximately 1% strain difference between its inside and outside surfaces. If the pitch line is in the center of the web and is nominally at 0.25% strain, the neutral axis will continue to experience 0.25% strain, the outer surface will experience 0.75% strain and the inner surface will experience 0.25% compression. Especially with thick webs, and considering times of peak tension, care must be taken to select a roller radius that does not cause damage to either of the web's surfaces due to over extension or compression.

PITCH RADIUS AND VELOCITY ERRORS

The web's neutral bending axis is also its pitch line as it traverses a roller. The velocity of the web approaching a roller is determined by its pitch line velocity. Assuming the pitch line is in the center of the web, the pitch line velocity is

$$V = \omega(r_o + h_w/2) \quad \{9\}$$

A web with a thickness profile, either natural or due to product design, will have a varying pitch line radius across its width and therefore a cross direction velocity profile. This is a potential cause of wrinkles and tracking error. The size of the velocity profile that can be tolerated depends on the nature of the web and cannot be easily determined. A larger roller radius will minimize the cross direction velocity profile that develops and minimizes the potential for wrinkles and mistracking.

AIR ENTRAINMENT

As a web traverses a roller a film of entrained air is trapped between the web and roller. The air film increases with velocity and at some point can separate enough of the

web from the roller surface that traction is lost. The initial air film thickness, h_a , can be calculated by the Knox-Sweeney equation

$$h_a = 0.643r_o \left[\frac{6\eta(V_{web} + V_{roller})}{T/l} \right]^{2/3} \quad \{10\}$$

Increasing the roller's radius increases the initial air film thickness and lowers the velocity at which separation occurs. The usual means of solving air entrainment problems is by adding texture or grooves to the roller surface to provide a path for the air to escape.

CRITICAL SPEED AND RPM

Critical speed and running RPM must be considered when sizing a roller. The critical speed depends on many factors in addition to the radius of the shell. However, considering just the shell alone, the first critical speed, ω_c , for a simply supported hollow shell is

$$\omega_c = \frac{k}{2\pi^2} \sqrt{\frac{IEI}{m}} \quad \{11\}$$

For the optimum 0.082 m shell in this example, the critical speed is almost 600 rev/s while its rotational speed is only 9.7 rev/s.

OTHER CONSIDERATIONS

Major considerations in idler design are cost and size. Radius is a factor in both. Larger idlers generally will cost more and can be a factor in determining the overall size of the machine that uses them, which may be a bigger cost than the idlers themselves.

Wall thickness of the idler tube should be as thin as possible to minimize the rotating mass with the limit being dent resistance and mechanical integrity.

Size of standard materials is a factor. The optimum 0.082 m radius in this example is not a standard size. Figure 5 shows that radii from 0.075 m to 0.1 m would have similarly small ΔT_{peak} values.

CONCLUSION

Typically idlers are sized based on deflection standards alone. Some industries consider the stress profiles through the thickness, but for thin, flexible webs, this is not usually a factor. Designing idlers to minimize their effect on tension becomes more important when equipment is designed for high acceleration, high speed, and low tension.

APPENDICES

Bearing + Inertial drag plotted as a function of radius and thickness

| Outside Radius = | 0.01 | 0.02 | 0.03 | 0.04 | 0.05 | 0.06 | 0.07 | 0.08 | 0.09 | 0.1 | 0.11 | 0.12 |
|-------------------------|--------|--------|--------|--------|--------|--------|--------|--------|--------|--------|--------|--------|
| Wall Thickness = 0.0005 | 15.512 | 4.0248 | 1.8707 | 1.1125 | 0.7625 | 0.5751 | 0.4652 | 0.3971 | 0.3535 | 0.3253 | 0.3073 | 0.2963 |
| 0.001 | 15.524 | 4.049 | 1.9075 | 1.1618 | 0.8244 | 0.6495 | 0.5522 | 0.4967 | 0.4657 | 0.4501 | 0.4446 | 0.4462 |
| 0.0015 | 15.535 | 4.0726 | 1.9436 | 1.2105 | 0.8857 | 0.7234 | 0.6386 | 0.5956 | 0.5772 | 0.5742 | 0.5813 | 0.5954 |
| 0.002 | 15.545 | 4.0955 | 1.9791 | 1.2585 | 0.9463 | 0.7966 | 0.7244 | 0.694 | 0.6881 | 0.6976 | 0.7173 | 0.744 |
| 0.0025 | 15.555 | 4.1178 | 2.014 | 1.306 | 1.0063 | 0.8691 | 0.8095 | 0.7917 | 0.7984 | 0.8205 | 0.8527 | 0.892 |
| 0.003 | 15.564 | 4.1395 | 2.0482 | 1.3528 | 1.0657 | 0.9411 | 0.894 | 0.8888 | 0.908 | 0.9427 | 0.9875 | 1.0393 |
| 0.0035 | 15.573 | 4.1605 | 2.0818 | 1.399 | 1.1244 | 1.0124 | 0.9779 | 0.9852 | 1.017 | 1.0643 | 1.1216 | 1.186 |
| 0.004 | 15.58 | 4.181 | 2.1148 | 1.4445 | 1.1825 | 1.0831 | 1.0612 | 1.081 | 1.1254 | 1.1852 | 1.2552 | 1.3321 |
| 0.0045 | 15.588 | 4.2007 | 2.1472 | 1.4894 | 1.24 | 1.1531 | 1.1438 | 1.1762 | 1.2332 | 1.3055 | 1.388 | 1.4776 |
| 0.005 | 15.594 | 4.2199 | 2.1789 | 1.5337 | 1.2969 | 1.2226 | 1.2258 | 1.2708 | 1.3403 | 1.4252 | 1.5203 | 1.6224 |
| 0.0055 | 15.6 | 4.2384 | 2.21 | 1.5774 | 1.3531 | 1.2914 | 1.3071 | 1.3647 | 1.4468 | 1.5443 | 1.6519 | 1.7666 |
| 0.006 | 15.606 | 4.2564 | 2.2405 | 1.6204 | 1.4087 | 1.3595 | 1.3879 | 1.458 | 1.5527 | 1.6627 | 1.7829 | 1.9102 |
| 0.0065 | 15.61 | 4.2736 | 2.2703 | 1.6629 | 1.4637 | 1.4271 | 1.468 | 1.5507 | 1.6579 | 1.7805 | 1.9133 | 2.0531 |
| 0.007 | 15.614 | 4.2903 | 2.2995 | 1.7046 | 1.5181 | 1.494 | 1.5475 | 1.6427 | 1.7625 | 1.8977 | 2.0431 | 2.1954 |
| 0.0075 | 15.618 | 4.3063 | 2.3281 | 1.7458 | 1.5718 | 1.5603 | 1.6263 | 1.7342 | 1.8665 | 2.0143 | 2.1722 | 2.3371 |
| 0.008 | 15.621 | 4.3217 | 2.3561 | 1.7863 | 1.6249 | 1.6259 | 1.7046 | 1.8249 | 1.9699 | 2.1302 | 2.3007 | 2.4782 |
| 0.0085 | 15.623 | 4.3365 | 2.3834 | 1.8262 | 1.6773 | 1.691 | 1.7822 | 1.9151 | 2.0726 | 2.2455 | 2.4285 | 2.6186 |
| 0.009 | 15.624 | 4.3506 | 2.4101 | 1.8655 | 1.7292 | 1.7554 | 1.8591 | 2.0046 | 2.1747 | 2.3602 | 2.5558 | 2.7584 |
| 0.0095 | 15.625 | 4.3641 | 2.4362 | 1.9041 | 1.7804 | 1.8192 | 1.9355 | 2.0936 | 2.2762 | 2.4742 | 2.6824 | 2.8976 |
| 0.01 | 15.626 | 4.377 | 2.4617 | 1.9421 | 1.831 | 1.8823 | 2.0112 | 2.1818 | 2.377 | 2.5876 | 2.8084 | 3.0361 |

Table 3 – Values of Total Drag vs. Radius and Wall Thickness